

# A MEASUREMENT OF $CP$ VIOLATION IN $B^0$ MESON DECAYS WITH BELLE

HIROAKI AIHARA

*Department of Physics, University of Tokyo,  
Tokyo 113-0033, Japan*

*E-mail:aihara@phys.s.u-tokyo.ac.jp*

Representing the Belle Collaboration

*To appear in the Proceedings of the XXXth International Conference on High Energy  
Physics July 27 - August 2, 2000 Osaka, Japan*

We present a preliminary measurement of the Standard Model  $CP$  violation parameter  $\sin 2\phi_1$  using the Belle detector. A  $6.2 \text{ fb}^{-1}$  sample of events produced by the KEKB asymmetric  $e^+e^-$  collider operating at the  $\Upsilon(4S)$  resonance is used. One neutral  $B$  meson is fully reconstructed via its decay to a  $CP$  eigenstate:  $J/\psi K_S$ ,  $\psi(2S)K_S$ ,  $\chi_{c1}K_S$ ,  $J/\psi K_L$  or  $J/\psi\pi^0$ . The flavor of the accompanying  $B$  is identified mainly from the charges of high momentum leptons or kaons among its decay products. The time interval between the two decays is determined from the distance between the decay vertices. A maximum likelihood fitting method is used to extract  $\sin 2\phi_1$  from the asymmetry in the time interval distribution. We report a preliminary result of

$$\sin 2\phi_1 = 0.45_{-0.44}^{+0.43}(\text{stat})_{-0.09}^{+0.07}(\text{syst}).$$

## 1 Introduction

The Belle experiment at the KEKB asymmetric energy  $e^+e^-$   $B$ -meson factory recently completed a successful first year of operation. The KEKB luminosity, which was about  $10^{31} \text{ cm}^{-2}\text{s}^{-1}$  at the time of startup in June 1999, reached a level of  $2 \times 10^{33} \text{ cm}^{-2}\text{s}^{-1}$  by July 2000. The Belle detector collected a total integrated luminosity of  $6.8 \text{ fb}^{-1}$ ,  $6.2 \text{ fb}^{-1}$  on the  $\Upsilon(4S)$  resonance and  $0.6 \text{ fb}^{-1}$  off resonance. We use this data sample to make a preliminary measurement of the Standard Model  $CP$  violation parameter  $\sin 2\phi_1$  using  $B_d^0 \rightarrow J/\psi K_S$ ,  $\psi(2S)K_S$ ,  $\chi_{c1}K_S$ ,  $J/\psi\pi^0$  and  $J/\psi K_L$  decays<sup>a</sup>.

The Standard Model predicts a  $CP$  violation through a mechanism of Spontaneous Symmetry Breaking of the electroweak symmetry that results in the Cabibbo-Kobayashi-Maskawa (CKM) quark mixing matrix. In systems of mesons containing a  $b$  quark,  $CP$

violating effects are expected to be large. The interference between the direct  $B_d^0 \rightarrow f_{CP}$  decay amplitude and the mixing-induced  $B_d^0 \rightarrow \bar{B}_d^0 \rightarrow f_{CP}$  decay amplitude, where  $f_{CP}$  is a  $CP$  eigenstate to which both  $B_d^0$  and  $\bar{B}_d^0$  can decay, gives rise to an asymmetry in the time-dependent decay rate:

$$\begin{aligned} A(t) &\equiv \frac{dN/dt(\bar{B}_{t=0}^0 \rightarrow f_{CP}) - dN/dt(B_{t=0}^0 \rightarrow f_{CP})}{dN/dt(\bar{B}_{t=0}^0 \rightarrow f_{CP}) + dN/dt(B_{t=0}^0 \rightarrow f_{CP})} \\ &= -\eta_f \sin 2\phi_1 \sin \Delta m_d t, \end{aligned} \tag{1}$$

where  $t$  is the proper time,  $dN/dt(\bar{B}_{t=0}^0 \rightarrow f_{CP})$  ( $B_{t=0}^0 \rightarrow f_{CP}$ ) is the decay rate for a  $\bar{B}^0$  ( $B^0$ ) produced at  $t = 0$  to decay to  $f_{CP}$  at time  $t$ ,  $\eta_f$  is a  $CP$ -eigenvalue of  $f_{CP}$ , ( $\eta_f = -1$  for  $J/\psi K_S$ ,  $\psi(2S)K_S$  and  $\chi_{c1}K_S$ , and  $+1$  for  $J/\psi\pi^0$  and  $J/\psi K_L$ ),  $\Delta m_d$  is the mass difference between two  $B^0$  mass eigenstates, and  $\phi_1$  is one of the three internal angles<sup>1</sup> of the CKM Unitarity Triangle, defined as  $\phi_1 \equiv \pi - \arg(\frac{-V_{ub}^* V_{td}}{-V_{cb}^* V_{cd}})$ .

In  $\Upsilon(4S)$  decays,  $B^0$  and  $\bar{B}^0$  mesons are pair-produced and remain in a coherent p-state until one of them decays. The decay

<sup>a</sup>Throughout this paper, when a mode is quoted the inclusion of a charge conjugate mode is implied unless otherwise stated.

of one  $B^0$  meson to a final state  $f_1$  at time  $t_1$  projects the accompanying  $B^0$  meson onto an orthogonal state at that time; this meson then propagates in time and decays to  $f_2$  at time  $t_2$ .  $CP$  violations can be measured if one of  $B$  mesons decays to a tagging state,  $f_{tag}$ , i.e. a final state unique to  $B^0$  or  $\overline{B}^0$ , at time  $t_{tag}$  and the other decays to an  $f_{CP}$  state at time  $t_{CP}$ . A time-dependent asymmetry,  $A(\Delta t)$ , which is obtained by replacing time  $t$  in (1) with the proper time interval  $\Delta t \equiv t_{CP} - t_{tag}$ , can then be observed in  $\Upsilon(4S)$  decays. Because the  $B^0\overline{B}^0$  pair is produced nearly at rest in the  $\Upsilon(4S)$  center of mass system (cms),  $\Delta t$  can be determined from the distance between  $f_{CP}$  and  $f_{tag}$  decay vertices in the boost ( $z$ ) direction,  $z_{CP}$  and  $z_{tag}$ , and  $\Delta t \sim \Delta z/\beta\gamma c$ , where  $\beta\gamma$  is a Lorentz boost factor of the  $\Upsilon(4S)$  restframe (equal to 0.425 at KEKB).

This asymmetry is diluted by experimental factors including background to the reconstructed  $f_{CP}$  states, the fraction of events where the flavor of the  $B$  meson is incorrectly tagged ( $\omega$ ), and the resolution of the decay vertex determination ( $d_{res}$ ):

$$A_{observed} = \left\{ \frac{1}{1 + B/S} (1 - 2\omega) d_{res} \right\} A = DA. \quad (2)$$

where  $B/S$  is the ratio of background<sup>b</sup> to signal and  $D(< 1)$  is the ‘‘dilution factor.’’ The statistical error of  $\sin 2\phi_1$  is inversely proportional to  $D$ :  $\delta \sin 2\phi_1 = \frac{1}{\sqrt{S+B}} \frac{1}{D}$ .

## 2 The Belle Detector

Belle is a large-solid-angle magnetic spectrometer<sup>2</sup>. Charged particle tracking is provided by a three-layer, double-sided silicon vertex detector (SVD) and a small-cell cylindrical drift chamber (CDC) consisting of 50 layers of anode wires, 18 of which are inclined at small angles. The tracking system is situated in a 1.5 T solenoidal field. The charged

particle acceptance is  $17^\circ < \theta < 150^\circ$ , where  $\theta$  is the polar angle in the laboratory frame with respect to the beam axis; the corresponding cms acceptance is  $\sim 92\%$  of the full solid angle. The impact parameter resolutions are  $\sigma_{r\phi}^2 = (21)^2 + \left(\frac{69}{p\beta \sin^{3/2}\theta}\right)^2 \mu\text{m}$  in the plane perpendicular to the beam axis, and  $\sigma_z^2 = (39)^2 + \left(\frac{51}{p\beta \sin^{3/2}\theta}\right)^2 \mu\text{m}$  along the beam direction, where  $p$  is the momentum measured in GeV/ $c$  and  $\beta$  is the velocity divided by  $c$ . The transverse momentum resolution is  $(\sigma_{p_t}/p_t)^2 = (0.0019p_t)^2 + (0.0034)^2$ . Charged hadron identification is provided by  $dE/dx$  measurements in the CDC, aerogel Cherenkov counters (ACC) and a barrel of 128 time-of-flight scintillation counters (TOF). The  $dE/dx$  measurements have a resolution for hadron tracks of  $\sigma(dE/dx) = 6.9\%$  and are useful for  $\pi/K$  separation for  $p < 0.8$  GeV/ $c$ . The TOF system has a time resolution of 95 ps (*rms*) and provides  $\pi/K$  separation for  $p < 1.5$  GeV/ $c$ . The indices of refraction of the ACC elements vary with polar angle from 1.01 to 1.03 to match the kinematics of the asymmetric energy collisions and provide  $\pi/K$  separation for  $1.5$  GeV/ $c < p < 3.5$  GeV/ $c$ . Particle identification probabilities are calculated from the combined response of the three systems. The efficiency for  $K^\pm$  is  $\sim 80\%$  with a charged pion fake rate of  $\sim 10\%$  for all momenta up to 3.5 GeV/ $c$ .

An array of 8736 CsI(Tl) crystals provides electromagnetic calorimetry that covers the same solid angle as the charged particle tracking system. The photon energy resolution, estimated from beam tests, is  $(\sigma_E/E)^2 = (0.013)^2 + (0.0007/E)^2 + (0.008/E^{1/4})^2$ , where  $E$  is measured in GeV. Neutral pions are detected via their decay to  $\gamma\gamma$ . The  $\pi^0$  mass resolution varies slowly with energy, averaging  $\sigma_{m_{\pi^0}} = 4.9$  MeV/ $c^2$ . With a  $\pm 3\sigma$  mass selection requirement, the overall detection efficiency, including geometric acceptance, for  $\pi^0$ s from  $B\overline{B}$  events is 40%. Electron identification is based on a

<sup>b</sup>Background in (2) is assumed to have no asymmetry.

combination of the CDC  $dE/dx$  information, the response of the ACC, and the position, shape and energy deposit of its associated CsI shower. The electron identification efficiency is above 90% for  $p > 1.0$  GeV/ $c$  with a pion fake rate that is below 0.5%.

The magnetic field is returned via an instrumented iron yoke consisting of alternating layers of resistive plate counters and 4.7 cm thick iron plates. The total iron thickness of 65.8 cm plus the material of the CsI calorimeter corresponds to 4.7 nuclear interaction lengths at normal incidence. This system, called the KLM, detects muons and  $K_L$  mesons in the region of  $20^\circ < \theta < 155^\circ$ . The overall muon identification efficiency is above 90% for  $p > 1$  GeV/ $c$  tracks detected in the CDC; a pion fake rate is below 2%.  $K_L$  mesons are identified by the presence of the KLM hits originating from hadronic interactions of the  $K_L$  in the CsI and/or iron. If there are CsI hits associated with a candidate  $K_L$ , its direction is determined from the energy-weighted center of gravity of the CsI hits alone. Otherwise, the direction is determined from the average position of the associated KLM hits. The angular resolution of the  $K_L$  direction is estimated to be  $\sim 1.5^\circ$  and  $\sim 3^\circ$  with and without associated CsI hits.

### 3 Selection of $B^0$ Decays to $CP$ Eigenstates

We reconstruct  $B^0$  decays to the following  $CP$  eigenstates<sup>3</sup>:  $J/\psi K_S$ ,  $\psi(2S)K_S$ ,  $\chi_{C1}K_S$  for  $CP - 1$  states and  $J/\psi\pi^0$ ,  $J/\psi K_L$  for  $CP + 1$  states. The  $B^0\bar{B}^0$  hadronic events are selected by requiring (i) at least three tracks with a minimum  $p_t$  of 0.1 GeV/ $c$  originating within 2.0 cm and 4.0 cm of the run-by-run average interaction point (IP) in the plane transverse to the beam axis ( $xy$  plane) and along the beam axis ( $z$  axis), respectively; (ii) at least two neutral energy clusters with a minimum energy of 0.1 GeV in the barrel

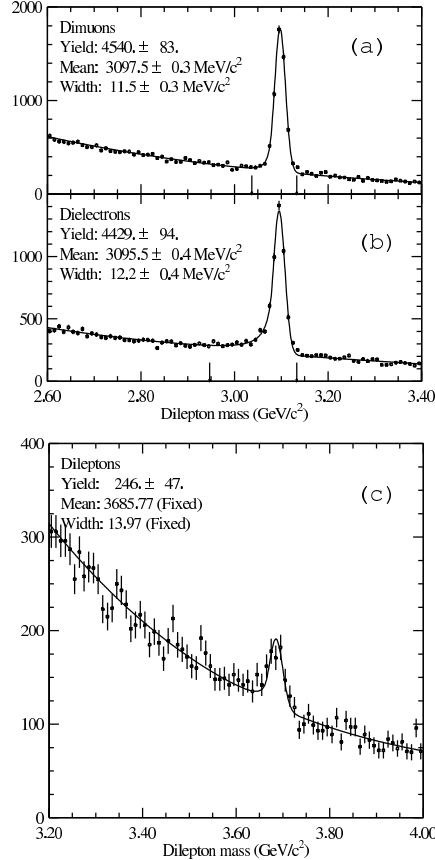


Figure 1. The invariant mass distributions for (a)  $J/\psi \rightarrow \mu^+\mu^-$ , (b)  $J/\psi \rightarrow e^+e^-$  and (c)  $\psi(2S) \rightarrow \mu^+\mu^-, e^+e^-$ .

CsI calorimeter; (iii) a sum of all CsI cluster energies that is between 10 % and 80 % of the cms energy ( $E_{\text{cms}}$ ); (iv) the total visible (charged and neutral) energy greater than 20 % of  $E_{\text{cms}}$ ; (v)  $|\sum p_z^{\text{cms}}|$  less than 50 % of  $E_{\text{cms}}/c$ , where  $p_z^{\text{cms}}$  is the  $z$  component of the momentum calculated in the cms frame; (vi) a reconstructed event vertex within 1.5 cm and 3.5 cm of the IP in the  $xy$  plane and along the  $z$  axis, respectively. In addition, we apply an event topology cut,  $H_2/H_0 \leq 0.5$ , where  $H_2$  and  $H_0$  are the second and zeroth Fox-Wolfram moments, to reject continuum background.

The  $J/\psi$  and  $\psi(2S)$  mesons are reconstructed via their decays to  $\mu^+\mu^-$  and  $e^+e^-$ .

Dimuon candidates are oppositely charged track pairs where at least one track is positively identified as a muon by the KLM system and the other is either positively identified as a muon or has a CsI energy deposit that is consistent with that of a minimum ionizing particle. Similarly, dielectron candidates are oppositely charged track pairs where at least one track is well identified as an electron and the other track satisfies at least the  $dE/dx$  or the CsI  $E/p$  electron identification requirements. For dielectron candidates, we correct for final state radiation or bremsstrahlung in the inner parts of the detector by including the four-momentum of every photon detected within 0.05 radian of the original electron direction in the  $e^+e^-$  invariant mass calculation. The invariant mass distributions for  $J/\psi \rightarrow \mu^+\mu^-$ ,  $J/\psi \rightarrow e^+e^-$  and  $\psi(2S) \rightarrow \mu^+\mu^-, e^+e^-$  are shown in Figs. 1(a), (b) and (c), respectively. The  $\psi(2S)$  is also reconstructed via its  $J/\psi\pi^+\pi^-$  decay and the  $\chi_{c1}$  is reconstructed through its decay to  $J/\psi\gamma$ . Figures 2 (a) and (b) show the mass difference distributions of  $M_{\ell^+\ell^-\pi^+\pi^-} - M_{\ell^+\ell^-}$  and  $M_{\ell^+\ell^-\gamma} - M_{\ell^+\ell^-}$ .

Candidate  $K_S \rightarrow \pi^+\pi^-$  decays are oppositely charged track pairs that have an invariant mass between 482 and 514  $\text{MeV}/c^2$ , which corresponds to the  $\pm 3\sigma$  around the  $K_S$  mass peak. The  $K_S \rightarrow \pi^0\pi^0$  decay mode is also used for the  $J/\psi K_S$  channel. These are selected among photons with a minimum energy of 50 MeV and 200 MeV in the barrel and endcap regions, respectively, by requiring, assuming  $K_S$  decayed at the IP, (i) a minimum  $\pi^0$  momentum of 100  $\text{MeV}/c$ ; (ii)  $118 < M_{\gamma\gamma} < 150 \text{ MeV}/c^2$ ; and (iii)  $300 < M_{\pi^0\pi^0} < 1000 \text{ MeV}/c^2$ . For each candidate, we determine the most probable  $K_S$  decay point by minimizing the sum of the  $\chi^2$  values from constraining each photon pair to  $\pi^0$  invariant mass while varying the  $K_S$  decay point along the  $K_S$  flight direction defined by the sum of four photon momenta and the IP. We then recalculate the invariant

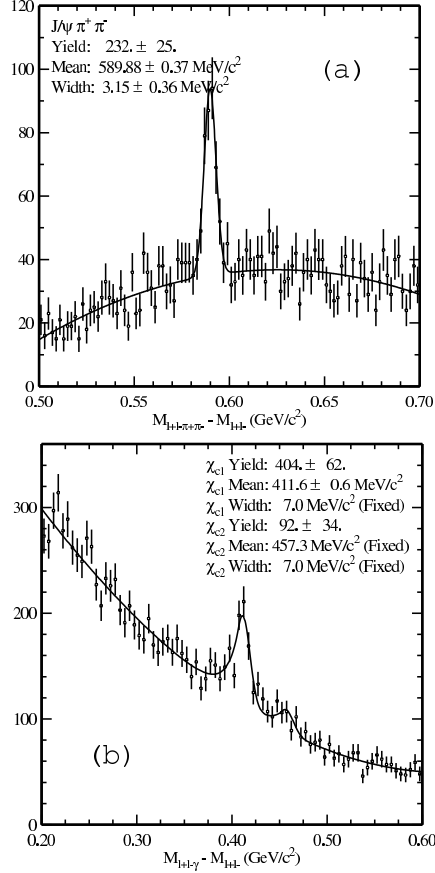


Figure 2. the mass difference distributions of (a)  $M_{\ell^+\ell^-\pi^+\pi^-} - M_{\ell^+\ell^-}$  and (b)  $M_{\ell^+\ell^-\gamma} - M_{\ell^+\ell^-}$ .

masses of the photon pairs and the  $\pi^0$ s and require the recalculated  $K_S$  mass to be between 470 and 520  $\text{MeV}/c^2$ . For the  $J/\psi\pi^0$  mode, the  $\pi^0$  candidates are selected from photons with a minimum energy of 100 MeV.

To identify reconstructed  $B$  meson decays we use the beam-constrained mass  $M_{beam} \equiv \sqrt{E_{beam}^2 - p_B^2}$  and the energy difference  $\Delta E \equiv E_B - E_{beam}$ , where  $E_{beam}$  is  $E_{cms}/2$  and  $p_B$  and  $E_B$  are the  $B$  candidate three-momentum and energy calculated in the cms. Figure 3 shows the  $M_{beam}$  distribution of the combined  $B \rightarrow J/\psi K_S(\pi^+\pi^-)$ ,  $J/\psi K_S(\pi^0\pi^0)$ ,  $\psi(2S)K_S(\pi^+\pi^-)$ ,  $\chi_{c1}K_S(\pi^+\pi^-)$ , and  $J/\psi\pi^0$

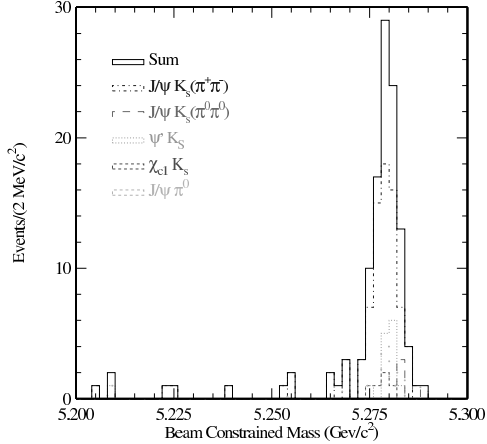


Figure 3. The beam-constrained mass distribution of sum of  $B \rightarrow J/\psi K_S(\pi^+\pi^-)$ ,  $J/\psi K_S(\pi^0\pi^0)$ ,  $\psi(2S)K_S(\pi^+\pi^-)$ ,  $\chi_{c1}K_S(\pi^+\pi^-)$ , and  $J/\psi\pi^0$  events.

samples, after the imposition of a  $3.5\sigma$  cut on  $|\Delta E|$  ( $\pm 40$  MeV for modes with  $K_S \rightarrow \pi^+\pi^-$  and  $\pm 100$  MeV for modes containing  $\pi^0$ s). The  $B$  meson signal region is defined as  $|M_{beam-} < M_{beam} >| < 0.01$   $\text{GeV}/c^2$ , where  $< M_{beam} >$  is the mean value of observed  $M_{beam}$ . Table 1 lists the number of signal candidates ( $N_{ev}$ ) and the backgrounds ( $N_{bkgd}$ ) determined from extrapolating the event rate in the non-signal  $\Delta E$  vs  $M_{beam}$  region into the signal region, and from the full Monte Carlo (MC) simulation results.

The  $B^0 \rightarrow J/\psi K_L$  event candidates are selected by requiring the  $J/\psi$  momentum and the  $K_L$  direction to be consistent with two-body-decay kinematics. After re-

Table 1. Summary of the reconstructed  $CP$  eigenstates

Mode	$N_{ev}$	$N_{bkgd}$
$J/\psi K_S(\pi^+\pi^-)$	70	3.4
$J/\psi K_S(\pi^0\pi^0)$	4	0.3
$\psi(2S)K_S(\pi^+\pi^-)$	5	0.2
$\psi(2S)(J/\psi\pi^+\pi^-)K_S(\pi^+\pi^-)$	8	0.6
$\chi_{c1}(\gamma J/\psi)K_S(\pi^+\pi^-)$	5	0.75
$J/\psi\pi^0$	10	1
Total	102	6.25

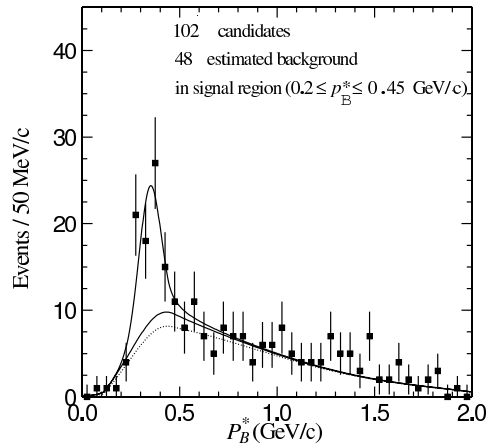


Figure 4. The  $p_B^*$  distribution with the results of the fit. The upper solid line is a sum of the signal and background. The total background (lower solid line) is divided into those coming from  $J/\psi K^*(K_L\pi^0)$  and  $J/\psi$  + non-resonant  $K_L\pi^0$  (above the dotted line) and those coming from all other sources (below the dotted line).

quiring the  $J/\psi$  cms momentum to be between 1.42 and 2.0  $\text{GeV}/c$ , we calculate the cms momentum of the  $B$  meson,  $p_B^*$ , which should be equal to  $\sim 0.34$   $\text{GeV}/c$  for a true event. Figure 4 shows the  $p_B^*$  distribution. Also shown are expected distributions of signal and background derived from the full MC simulation studies. The background is found to be dominated by  $B \rightarrow J/\psi X$  events including  $B \rightarrow J/\psi K^*(K_L\pi^0)$  and  $B \rightarrow J/\psi$  + non-resonant  $K_L\pi^0$ , which are a mixture of  $CP+1$  and  $CP-1$  eigenstates. There are 102  $J/\psi K_L$  candidates in the signal region defined as  $0.2 \leq p_B^* \leq 0.45$   $\text{GeV}/c$ . By fitting the data with the expected shapes, we find 48 background events in the signal region, of which 8 events were from  $J/\psi K^*(K_L\pi^0)$  +  $J/\psi$  non-resonant  $K_L\pi^0$ .

## 4 Flavor Tagging

Each event with a  $CP$  eigenstate is examined to see if the rest of the event, defined as the tag side ( $f_{tag}$ ), contains a signature specific to  $B^0$  or  $\bar{B}^0$ . Our tagging methods are

based on the correlation between the flavor of the decaying  $B$  mesons and the charge of a prompt leptons in  $b \rightarrow c\nu\ell$  decays, the charge of Kaon originating from  $b \rightarrow c \rightarrow s$  decays, or the charge of  $\pi$  from  $B \rightarrow D^*(\rightarrow \pi D)\ell\nu$  decays. A  $B^0(\overline{B}^0)$  flavor for  $f_{tag}$  indicates that  $f_{CP}$  was in  $\overline{B}^0(B^0)$  state at  $\Delta t = 0$ . We applied the following four tagging methods in descending order: if the event failed the method (1), we tested the event with the method (2), etc.

1. High momentum lepton: If  $f_{tag}$  contains a lepton ( $\ell^\pm = e^\pm$  or  $\mu^\pm$ ) with cms momentum  $p^* \geq 1.1$  GeV/ $c$ , we assign  $f_{tag} = B^0(\overline{B}^0)$  for  $\ell^+(\ell^-)$ .
2. Charged Kaon: If  $f_{tag}$  contains no high momentum  $\ell^\pm$ , the sum of the charges of all identified Kaons,  $Q_K$ , in  $f_{tag}$  is determined. We assign  $f_{tag} = B^0(\overline{B}^0)$  if  $Q_K > 0$  ( $Q_K < 0$ ). If  $Q_K = 0$ , the event fails this method.
3. Medium momentum lepton: If  $f_{tag}$  contains an identified lepton in the cms momentum range  $0.6 \leq p_\ell^* < 1.1$  GeV/ $c$ , we use the cms missing momentum ( $p_{miss}^*$ ) as an approximation of the  $\nu$  cms momentum. If  $p_\ell^* + p_{miss}^* \geq 2.0$  GeV/ $c$ , we assume  $f_{tag}$  is from  $b \rightarrow c\nu\ell$  decay and assign its flavor based on the charge of  $\ell$  as in the method (1).
4. Soft pion: If  $f_{tag}$  contains a low momentum ( $p^* < 200$  MeV/ $c$ ) charged track consistent with being a  $\pi$  from the  $D^* \rightarrow D\pi$  decay chain, we assign  $f_{tag} = B^0(\overline{B}^0)$  for  $\pi^-$  ( $\pi^+$ ).

The efficiency ( $\epsilon$ ) and the wrong tag fraction ( $\omega$ ) are determined using a sample of exclusively reconstructed  $B^0 \rightarrow D^*(D^-)\ell^+\nu$  decays which are self-tagging decay modes, and the full MC simulation. Because of  $B^0 - \overline{B}^0$  mixing, the probabilities of finding the opposite flavor ( $OF$ ) and same flavor ( $SF$ ) neutral

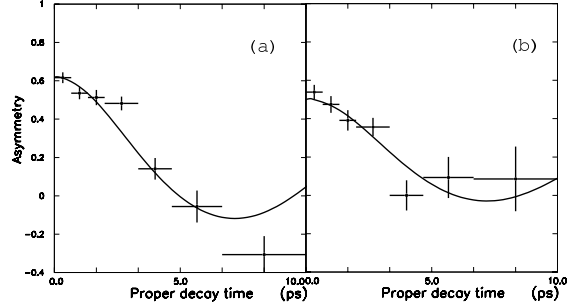


Figure 5. The  $B^0 - \overline{B}^0$  mixing amplitude as a function of the proper-time interval  $\Delta t$  of two neutral  $B$  mesons obtained using (a)  $B^0 \rightarrow D^*\ell\nu$  decays and (b)  $B^0 \rightarrow D\ell\nu$  decays. Also shown are the results of the fit (solid lines). We obtained  $\Delta m_d = 0.488 \pm 0.026$  ps $^{-1}$ .

Table 2. Tagging efficiency ( $\epsilon$ ) and wrong tag fraction ( $\omega$ )

Method	$\epsilon$	$\omega$
High $p^* \ell$	$0.0142 \pm 0.021$	$0.071 \pm 0.045$
$K^\pm$	$0.279 \pm 0.042$	$0.199 \pm 0.070$
Med. $p^* \ell$	$0.029 \pm 0.015$	$0.29 \pm 0.15$
Soft $\pi$	$0.070 \pm 0.035$	$0.34 \pm 0.15$

$B$  meson pairs are

$$\begin{aligned} P_{OF}(\Delta t) &\propto 1 + (1 - 2\omega) \cos(\Delta m_d \Delta t) \\ P_{SF}(\Delta t) &\propto 1 - (1 - 2\omega) \cos(\Delta m_d \Delta t). \end{aligned} \quad (3)$$

Therefore,  $\omega$  can be determined from the measurement of the  $B^0 - \overline{B}^0$  oscillation amplitude:

$$A_{mix} \equiv \frac{P_{OF} - P_{SF}}{P_{OF} + P_{SF}} = (1 - 2\omega) \cos(\Delta m_d \Delta t). \quad (4)$$

The flavor of one of the two neutral  $B$  mesons is identified using  $B^0 \rightarrow D^{*-}\ell^+\nu$  where  $D^{*-}$  decays to  $\overline{D}^0\pi^-$  followed by  $\overline{D}^0$  decays to either  $K^+\pi^-$ ,  $K^+\pi^-\pi^0$ , or  $K^+\pi^+\pi^-\pi^-$ , or using  $B^0 \rightarrow D^-\ell^+\nu$  where  $D^-$  decays to  $K^+\pi^-\pi^-$ . We then identify the flavor of the accompanying  $B$  meson by applying the tagging methods described above. The vertex position of  $D^*\ell\nu$  is determined by requiring the  $\ell$  track and the reconstructed  $D$  momentum vector form a common vertex. The ver-

Table 3. Summary of tagged events

$f_{CP}$	$N_{ev}$
$J/\psi K_S(\pi^+\pi^-)$	40
$J/\psi K_S(\pi^0\pi^0)$	4
$\psi(2S)K_S(\pi^+\pi^-)$	2
$\psi(2S)(J/\psi\pi^+\pi^-)K_S(\pi^+\pi^-)$	3
$\chi_{c1}(\gamma J/\psi)K_S(\pi^+\pi^-)$	3
$J\psi\pi^0$	4
$J/\psi K_L$	42
Total	98

tex position of the tagging  $B$  meson is determined using the method described in the next section. The proper-time interval  $\Delta t$  of two neutral mesons is derived from the distance between the two decay vertices. We obtain  $\omega$  and  $\Delta m_d$  from a fit to the  $\Delta t$  distributions of the  $OF$  and  $SF$  events with the expected functions, which include the effects of the  $\Delta t$  resolution and background. We determine  $\Delta m_d = 0.488 \pm 0.026 \text{ ps}^{-1}$ , which is in good agreement with the world average<sup>5</sup>. Figure 5 shows the measured  $A_{mix}$  distributions together with the fitted functions.

Table 2 summarizes the tagging efficiency and the wrong tag fractions. The total tagging efficiency is measured to be 0.52, and the total effective tagging efficiency ( $\epsilon_{eff}$ ), defined as a sum of  $\epsilon(1 - 2\omega)^2$  over all tagging methods, is 0.22. The statistical error on  $\sin 2\phi_1$  is proportional to  $1/\sqrt{\epsilon_{eff}}$ . Table 3 lists the number of tagged events for each  $f_{CP}$ . We find a total of 98 tagged events, of which 14 events were tagged by a high momentum  $e$ , 12 by a high momentum  $\mu$ , 48 by  $K^\pm$ , 3 by a medium momentum  $e$ , 3 by a medium momentum  $\mu$ , and 18 by a soft  $\pi$ .

## 5 Proper-time Interval Reconstruction

The  $f_{CP}$  vertex is determined with the two lepton tracks from  $J/\psi$ . We require that at least one of two tracks must have SVD hits and that the vertex point is consistent with

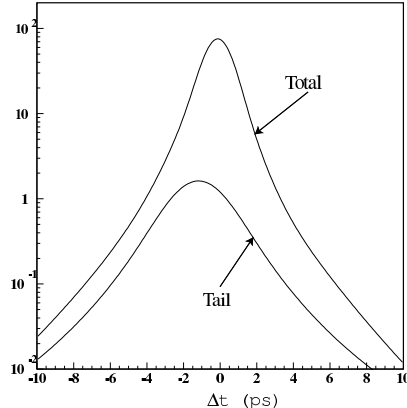


Figure 6. The average shape of the event-by-event resolution function obtained by summing over 300  $B^\pm \rightarrow J/\psi K^\pm$  events.

the IP profile. The  $f_{tag}$  vertex is formed from the remaining tracks in the event. In order to reduce the bias due to long-lived particles, tracks are excluded from the fit: if when combined with any other charged track they form an invariant mass consistent with a  $K_S$ ; if the track has a large tracking error in  $z$  direction ( $\sigma_z > 0.5 \text{ mm}$ ); or if the minimum distance between the track and the reconstructed  $f_{CP}$  vertex is too large,  $\delta z > 1.8 \text{ mm}$  or  $\delta r > 0.5 \text{ mm}$  (in the  $r\phi$  plane). In addition, the track with the worst  $\chi^2$  is removed from the fit if the reduced  $\chi^2$  of the vertex fit is more than 20. This procedure is iterated until the reduced  $\chi^2$  is below 20. The expected vertex resolutions are  $\sim 40 \mu\text{m}$  and  $\sim 85 \mu\text{m}$  for the  $f_{CP}$  and  $f_{tag}$  vertices, respectively.

The most probable  $\Delta t$  is estimated as  $\Delta z/\beta\gamma c$ . The resolution of  $\Delta t$ ,  $R(\Delta t)$ , is parameterized as a sum of two Gaussians, a *main* Gaussian arising from the intrinsic SVD resolution and the  $f_{tag}$  vertex smearing due to the finite lifetime of secondary charmed mesons, and a *tail* Gaussian due to a few poorly measured tracks:

$$R(\Delta t) = \frac{f_{main}}{\sigma\sqrt{2\pi}} \exp\left(-\frac{(\Delta t - \mu)^2}{2\sigma^2}\right) + \frac{f_{tail}}{\sigma_{tail}\sqrt{2\pi}} \exp\left(-\frac{(\Delta t - \mu_{tail})^2}{2\sigma_{tail}^2}\right). \quad (5)$$

The mean values ( $\mu$ ,  $\mu_{tail}$ ) and widths ( $\sigma$ ,  $\sigma_{tail}$ ) of the two Gaussians are calculated event-by-event from the  $f_{CP}$  and  $f_{tag}$  vertex errors, taking into account the error due to the approximation of  $\Delta t \sim \Delta z/\beta\gamma c$ . The Gaussian parameters and  $f_{tail}(=1-f_{main})$  are determined from the full MC simulation studies and a multi-parameter fit to  $B \rightarrow D^*\ell\nu$  data. In addition, by measuring the lifetime of the  $D^0 \rightarrow K^-\pi^+$  decays using only  $z$  coordinate information, we studied the intrinsic  $z$  vertex resolution. In order to show the average shape of the  $R(\Delta t)$ , Fig. 6 was drawn by summing event-by-event  $R(\Delta t)$  functions over 300  $B^\pm \rightarrow J/\psi K^\pm$  (real) events. The width of  $R(\Delta t)$  is dominated by the main Gaussian ( $f_{main} = 0.96 \pm 0.04$ ); we find  $\langle \sigma \rangle \sim 1.11$  ps,  $\langle \sigma_{tail} \rangle \sim 2.24$  ps,  $\langle \mu \rangle = -0.19$  ps, where  $\langle \rangle$  indicates the average over all events. (The  $\mu_{tail}$  was fixed to  $-1.25$  ps based on the simulation studies.) The non-zero negative mean values of the Gaussians reflect the bias in  $f_{tag}$  vertex position due to secondary charmed mesons.

Based on the above described vertex reconstruction and resolution function, we measured lifetimes of neutral and charged  $B$  mesons<sup>4</sup>. Figure 7 shows  $\Delta t$  distributions of some of measured decay modes with the results of the lifetime fit. Table 4 summarizes the results. The obtained values for different decay modes are consistent with each other and are in good agreement with the world averages<sup>5</sup>,  $\tau_{B^0} = 1.548 \pm 0.032$  ps, and  $\tau_{B^\pm} = 1.653 \pm 0.028$  ps. This verifies the validity of our  $\Delta z$  measurement and  $R(\Delta t)$ .

## 6 Extraction of $\sin 2\phi_1$

An unbinned maximum likelihood method is used to extract the best value for  $\sin 2\phi_1$ . The probability density function expected for the signal distribution with a  $CP$  eigenvalue of

Table 4. Summary of  $B$  meson lifetime measurements

Decay mode	lifetime (ps)
$\overline{B}^0 \rightarrow D^{*+}\ell^-\nu$	$1.50 \pm 0.06^{+0.06}_{-0.04}$
$\overline{B}^0 \rightarrow D^{*+}\pi^-$	$1.55^{+0.18+0.10}_{-0.17-0.07}$
$\overline{B}^0 \rightarrow D^+\pi^-$	$1.41^{+0.13}_{-0.12} \pm 0.07$
$\overline{B}^0 \rightarrow J/\psi\overline{K}^{*0}$	$1.56^{+0.22+0.09}_{-0.19-0.15}$
Combined	$1.50 \pm 0.05 \pm 0.07$
$\overline{B}^0 \rightarrow J/\psi K_S$	$1.54^{+0.28+0.11}_{-0.24-0.19}$
$\overline{B}^0 \rightarrow J/\psi K_L$	$1.28^{+0.36}_{-0.35}$
$B^- \rightarrow D^{*0}\ell^-\overline{\nu}$	$1.54 \pm 0.10^{+0.14}_{-0.07}$
$B^- \rightarrow D^0\pi^-$	$1.73 \pm 0.10 \pm 0.09$
$B^- \rightarrow J/\psi K^-$	$1.87^{+0.13+0.07}_{-0.12-0.14}$
Combined	$1.70 \pm 0.06^{+0.11}_{-0.10}$

$\eta_f$  is given by:

$$Sig(\Delta t, \eta_f, q) = \frac{1}{\tau_{B^0}} \exp(-|\Delta t|/\tau_{B^0}) \times \{1 - q(1 - 2\omega)\eta_f \sin 2\phi_1 \sin(\Delta m_d \Delta t)\}, \quad (6)$$

where  $q = 1(-1)$  if  $f_{tag} = B^0(\overline{B}^0)$  and  $\omega$  depends on the method of the flavor tagging as given in Table 2. The values of  $\tau_{B^0}$  and  $\Delta m_d$  are fixed to the world averages<sup>5</sup>,  $1.548 \pm 0.032$  ps and  $0.472 \pm 0.017$  ps<sup>-1</sup>, respectively. By investigating events in background-dominated regions (the side bands in the  $\Delta E$  vs  $M_{beam}$  scatterplot), we find that the probability density function for background events for all  $f_{CP}$  events (except for  $B^0 \rightarrow J/\psi K_L$  events) is consistent with  $Bkg(\Delta t) = \frac{1}{2\tau_{bkg}} \exp(-|\Delta t|/\tau_{bkg})$ , where  $\tau_{bkg} = 0.73 \pm 0.12$  ps. The likelihood of an event,  $i$ , is calculated as:

$$\rho_i = p_{sig} \int_{-\infty}^{+\infty} Sig(s, \eta_f, q) R(\Delta t - s) ds + (1 - p_{sig}) \int_{-\infty}^{+\infty} Bkg(s) R(\Delta t - s) ds, \quad (7)$$

where  $p_{sig}$  is the probability for the event being a signal, and  $R(\Delta t)$  is the resolution function described in the previous section. The log-likelihood  $-\sum_i \ln \rho_i$  is calculated by summing over all signal events. The most probable  $\sin 2\phi_1$  value is found by scanning over  $\sin 2\phi_1$  values to minimize the log-



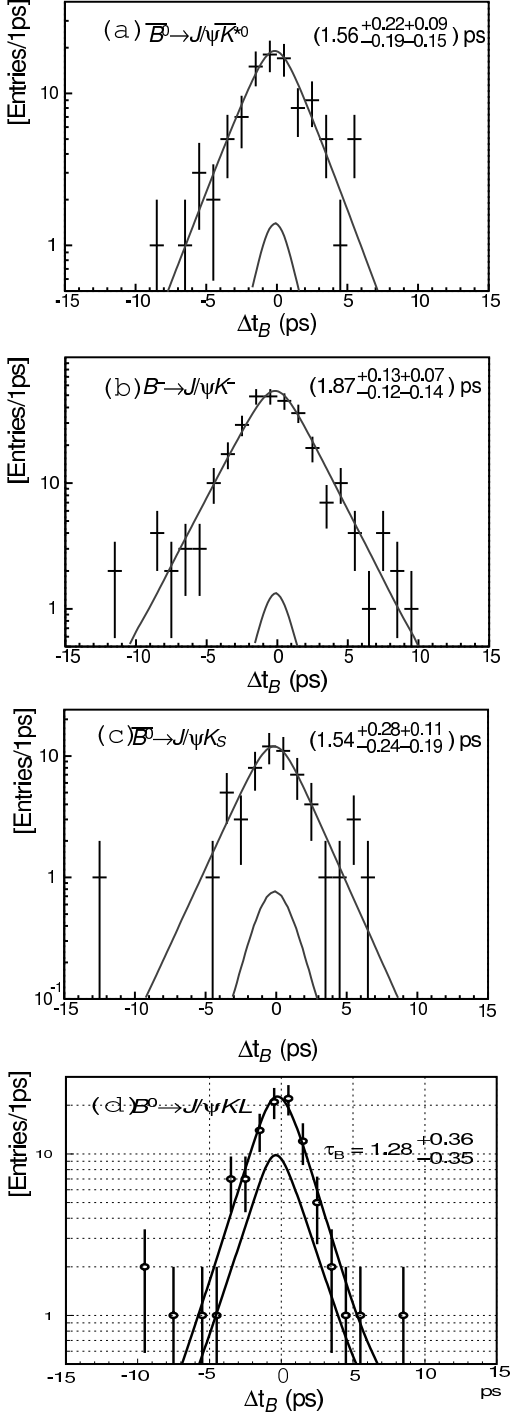


Figure 7.  $\Delta t$  distributions and the results of the lifetime fit for (a)  $\overline{B}^0 \rightarrow J/\psi \overline{K}^{*0}$ , (b)  $B^- \rightarrow J/\psi K^-$ , (c)  $\overline{B}^0 \rightarrow J/\psi K_S$  and (d)  $\overline{B}^0 \rightarrow J/\psi K_L$ . The lower solid curve represents the background distribution.

Table 5. Results of  $CP$  fit to control data.

Decay mode	Apparent $\sin 2\phi_1$
$\overline{B}^0 \rightarrow J/\psi (K^+ \pi^-)^{*0}$	$-0.094^{+0.492}_{-0.458}$
$B^- \rightarrow J/\psi K^-$	$+0.215^{+0.232}_{-0.238}$
$B^- \rightarrow D^0 \pi^-$	$-0.096 \pm 0.174$
$B^0 \rightarrow D^{*-} \ell^+ \nu$	$+0.09 \pm 0.18$

Table 6. Results of  $CP$  fit to tagged  $f_{CP}$  events.

Decay mode	$\sin 2\phi_1$
$J/\psi K_S (\pi^+ \pi^-)$ only	$+0.49^{+0.53}_{-0.57}$
All $CP - 1$ modes	$+0.81^{+0.44}_{-0.50}$
All $CP + 1$ modes	$-0.61^{+0.87}_{-0.78}$
All combined	$+0.45^{+0.43}_{-0.44}$

likelihood function.

To test for possible bias in the analysis, we apply the same analysis program including tagging, vertexing and log-likelihood fitting to control data samples with null intrinsic asymmetry:  $B^0 \rightarrow J/\psi K^{*0} (K^{*0} \rightarrow K^+ \pi^-)$ ;  $B^- \rightarrow J/\psi K^-$ ;  $B^- \rightarrow D^0 \pi^-$ ; and  $B^0 \rightarrow D^{*-} \ell^+ \nu$  decays. Figure 8 shows the  $\Delta t$  distributions of  $B^0 \rightarrow J/\psi K^{*0} (K^{*0} \rightarrow K^+ \pi^-)$ ,  $B^- \rightarrow J/\psi K^-$ , and  $B^- \rightarrow D^0 \pi^-$  events. The results of the fit for apparent  $CP$  asymmetry are given in Table 5; they are all consistent with null asymmetry. The results of the fit to the tagged  $f_{CP}$  events are summarized in Table 6. To display the fitted results, the  $dN/d\Delta t$  distribution for  $q = +1$  events and  $dN/d(-\Delta t)$  distribution for  $q = -1$  events are added:

$$\begin{aligned}
 & dN/d\Delta t|_{q=+1} + dN/d(-\Delta t)|_{q=-1} \\
 & \propto \exp(-|\Delta t|/\tau_{B^0}) \\
 & \times \{1 - (1 - 2\omega)\eta_f \sin 2\phi_1 \sin(\Delta m_d \Delta t)\}.
 \end{aligned} \tag{8}$$

Figures 9 (a) and (b) show the results for only  $f_{CP} = J/\psi K_S (\pi^+ \pi^-)$  events and for all  $CP - 1$  events combined. Figure 9 (c) shows the result for  $CP + 1$  events, i.e.  $J/\psi K_L$  and  $J/\psi \pi^0$ . In fitting to  $f_{CP} = J/\psi K_L (K_L \pi^0) + \text{non-resonant } J/\psi K_L \pi^0$ , which amounts to  $\sim 17\%$  of the total background, is taken to

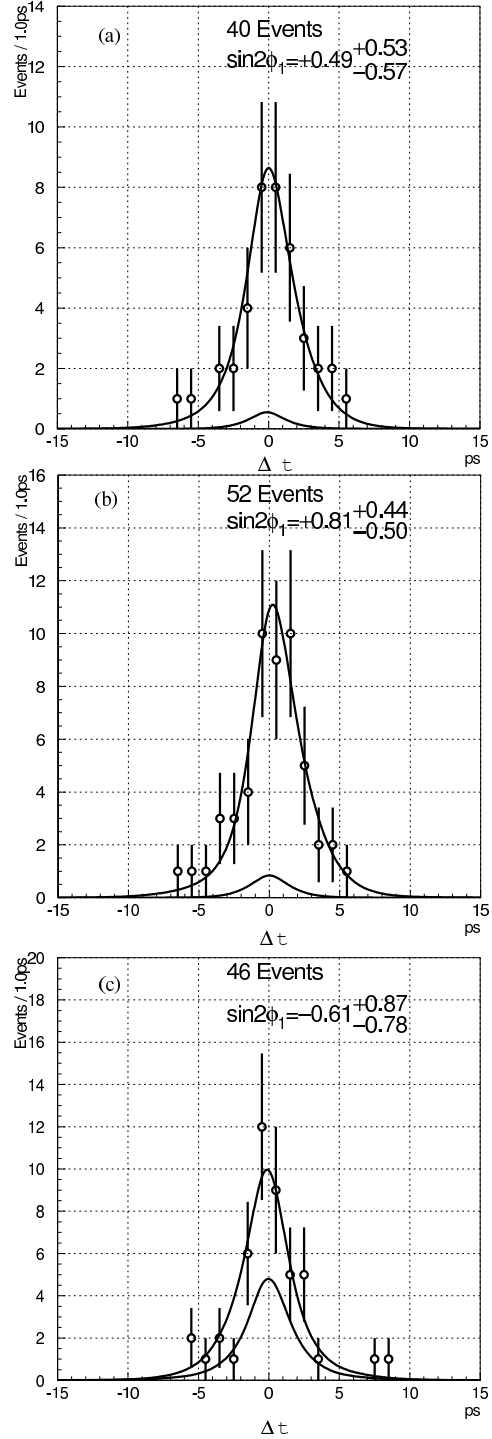
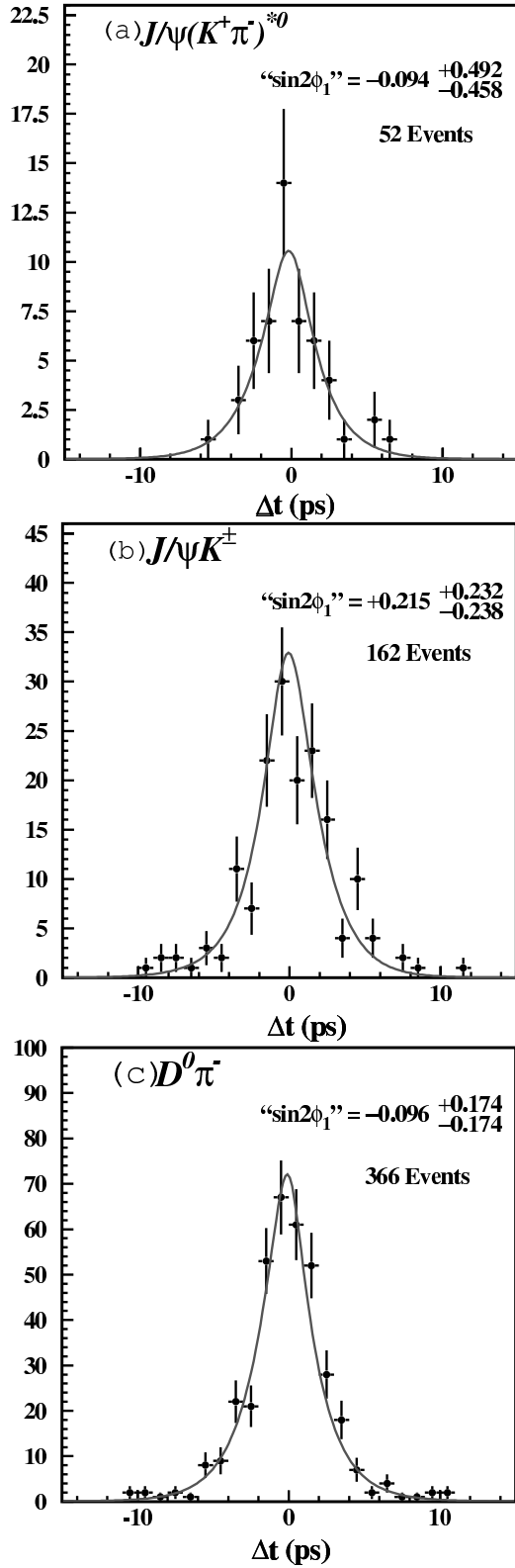


Figure 9.  $dN/d\Delta t|_{q=+1} + dN/d(-\Delta t)|_{q=-1}$  distributions and the results of the  $CP$  fit for (a)  $B^0 \rightarrow J/\psi K_S(\pi^+\pi^-)$  only, (b) all  $CP-1$   $f_{CP}$  modes combined, and (c) all  $CP+1$   $f_{CP}$  modes combined. A lower solid line in each figure indicates background contribution.

Figure 8.  $\Delta t$  distributions and the results of the  $CP$  fit for (a)  $B^0 \rightarrow J/\psi K^*(K^{*0} \rightarrow K^+\pi^-)$ , (b)  $B^- \rightarrow J/\psi K^\pm$ , and (c)  $B^- \rightarrow D^0\pi^-$  events.

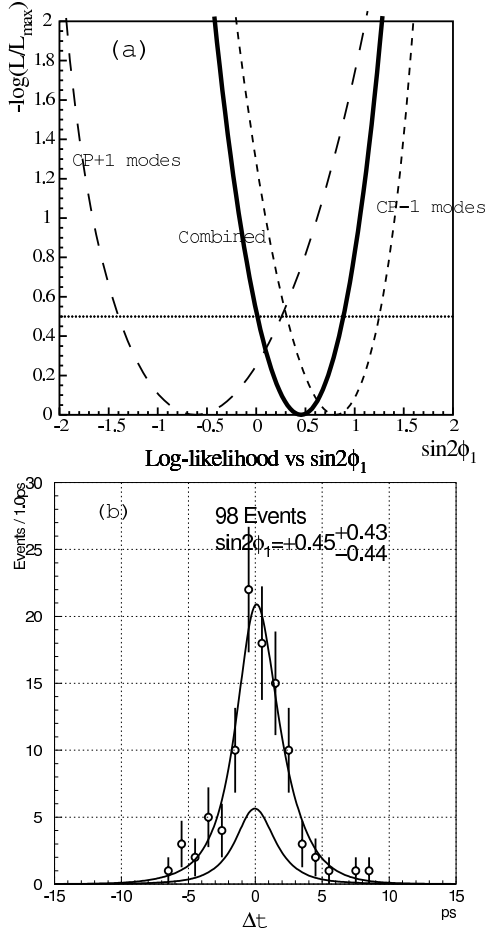


Figure 10. The log-likelihood as a function of  $\sin 2\phi_1$  (a) and a sum of  $dN/d(+\Delta t)|_{q=+1} + dN/d(-\Delta t)|_{q=-1}$  for  $\eta_f = -1$  and  $dN/d(-\Delta t)|_{q=+1} + dN/d(+\Delta t)|_{q=-1}$  for  $\eta_f = +1$  (b) for combined  $CP - 1$  and  $CP + 1$  events.

be a mixture of  $CP - 1$  (73%) and  $CP + 1$  (27%) states, based on the results of a  $B \rightarrow J/\psi K_S \pi^0$  analysis<sup>6</sup>. A fit to 52 events in the  $J\psi K_L$  sideband (i.e.  $1.0 < p_B^* < 2.0$  GeV/ $c$  region), where the non- $CP$   $J/\psi X$  events dominate, gives the result  $\sin 2\phi_1 = +0.02^{+0.48}_{-0.49}$ , consistent with null asymmetry. Finally we perform the simultaneous fit to  $CP - 1$  and  $CP + 1$  events to extract the best  $\sin 2\phi_1$  value. Figure 10 (a) shows the log-likelihood as a function of  $\sin 2\phi_1$  for a total of 98  $CP - 1$  and  $CP + 1$  combined events together with the results for  $CP - 1$  and  $CP + 1$  separately. We find  $\sin 2\phi_1 = +0.45^{+0.43}_{-0.44}$ . To display the results of the fit,  $dN/d(+\Delta t)|_{q=+1} + dN/d(-\Delta t)|_{q=-1}$  for  $\eta_f = -1$  and  $dN/d(-\Delta t)|_{q=+1} + dN/d(+\Delta t)|_{q=-1}$  for  $\eta_f = +1$  are added so that the distribution becomes approximately proportional to  $\exp(-|\Delta t|/\tau_{B^0})\{1 + (1 - 2\omega) \sin 2\phi_1 \sin(\Delta m_d \Delta t)\}$ , as shown in Fig. 10 (b).

We generated 1000 toy Monte Carlo experiments with the same number of tagged  $CP$  events, having the same composition of the tags and the same resolutions as in the  $CP$  data sample, for an input value of  $\sin 2\phi_1 = 0.45$ . Figures 11 (a) and (b) show the distributions of the central  $\sin 2\phi_1$  value and the statistical errors, + side and - side separately. We found that the probability of obtaining a value of the statistical error greater than the observed value was  $\sim 5\%$ .

Table 7 lists systematic errors. The largest error is due to uncertainty in the wrong tag fraction determination. This was studied by varying  $\omega$  individually for each tagging method. The effect due to uncertainty in  $\Delta t$  resolutions for both signal and background was studied by varying parameters in  $R(\Delta t)$ . Also included are the effects due to uncertainties in estimate of the background fraction, in the world average  $\tau_B$  and  $m_d$  values. An imperfect knowledge of the event-by-event IP profile could cause a systematic error in  $\sin 2\phi_1$  due to the vertex re-

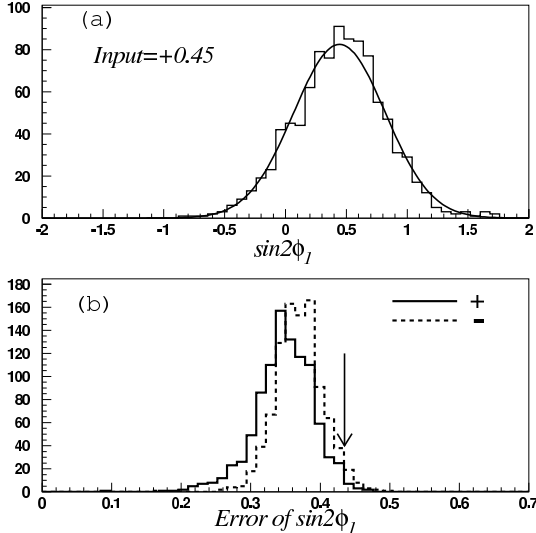


Figure 11. Results of 1000 toy Monte Carlo experiments generated for  $\sin 2\phi_1 = 0.45$ : distributions of the fitted  $\sin 2\phi_1$  (a) and statistical errors (b). In (b) distributions for errors on + side and - side are shown separately. Each experiment contains 98 events with the same tag composition as the real data.

construction. The effect was studied by repeating the entire fitting procedure by varying the IP envelope by  $\pm 1\sigma$  in all 3 dimensions. The total systematic error of  $\sin 2\phi_1$  is found to be  $+0.07 - 0.09$ .

## 7 Conclusion

Based on a  $6.2 \text{ fb}^{-1}$  data sample collected at the  $\Upsilon(4S)$  resonance during the first year of the KEKB operation, we made a preliminary determination of  $\sin 2\phi_1$  using 98 flavor-tagged events consisting of 40  $J/\psi K_S(\pi^+\pi^-)$ , 4  $J/\psi K_S(\pi^0\pi^0)$ , 5  $\psi(2S)K_S(\pi^+\pi^-)$ , 3  $\chi_{C1}K_S(\pi^+\pi^-)$ , 4  $J/\psi\pi^0$  and 42  $J/\psi K_L$  events. We found

$$\sin 2\phi_1 = 0.45_{-0.44}^{+0.43}(\text{stat})_{-0.09}^{+0.07}(\text{syst}).$$

Table 7. List of systematic errors of  $\sin 2\phi_1$

Source	$\sigma+$	$\sigma-$
Wrong tag	0.050	-0.066
$R(\Delta t)$	0.026	-0.025
Background shape	0.029	-0.042
Background fraction	0.029	-0.032
$\tau_{B^0}, \Delta m_d$	0.005	-0.006
IP profile	0.004	-0.000
Total	+0.07	-0.09

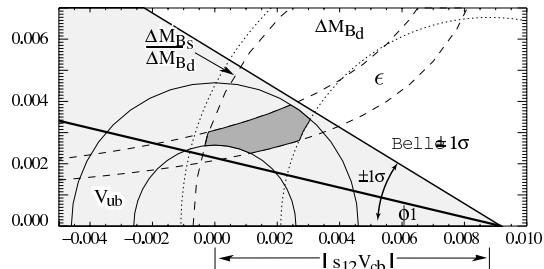


Figure 12. The region in the  $\rho - \eta$  plane corresponding to this measurement  $\pm 1\sigma$ ,  $\sin 2\phi_1 = 0.45_{-0.45}^{+0.44}$ . This was made by modifying Fig. 11.2 of ref. [5].

Figure 12 shows the region in the  $\rho - \eta$  plane<sup>c</sup> corresponding to this measurement  $\pm 1\sigma$ ,  $\sin 2\phi_1 = 0.45_{-0.45}^{+0.44}$ , together with the constraints derived from other measurements<sup>5</sup>. While the current statistical uncertainty does not allow anything conclusive, this preliminary result is consistent with the Standard Model prediction.

## Acknowledgments

We are grateful to the conference organizers for their hospitality. It is a pleasure to thank the KEKB group and the KEK computing research center. We acknowledge support from the Ministry of Education, Science, Sports

<sup>c</sup>The  $\rho - \eta$  plane is the complex plane of the triangle formed by the CKM matrix elements  $V_{ub}^*$ ,  $V_{td}$ , and  $s_{12}V_{cb}^*$ , rescaled by a factor of  $1/|s_{12}V_{cb}|$  so that the base is the unit length. The coordinates of the vertices of the unitarity triangle are  $A(\rho, \eta)$ ,  $B(1, 0)$  and  $C(0, 0)$ .

and Culture of Japan and the Japan Society for the Promotion of Science; the Australian Research Council and the Australian Department of Industry, Science and Resources; the Department of Science and Technology of India; the BK21 program of the Ministry of Education of Korea and the Basic Science program of the Korea Science and Engineering Foundation; the Polish State Committee for Scientific Research; the Ministry of Science and Technology of Russian Federation; the National Science Council and the Ministry of Education of Taiwan; the Japan-Taiwan Cooperative Program of the Interchange Association; and the U.S. Department of Energy.

## References

1. H. Quinn and A.I. Sanda, Eur.Phys.J. C **15**, 625 (2000).
2. Belle Collaboration, "The Belle Detector," to be submitted to Nucl.Instr. and Methods.
3. S. Schrenk (Belle Collaboration), "Studies of  $B$  Meson Decays to Final States Containing Charmonium with Belle," in this Proceedings.
4. H. Tajima (Belle Collaboration), "Measurement of Heavy Meson Lifetimes with Belle," *ibid.*
5. Particle Data Group, D.E. Groom *et al.*, Eur.Phys.J. C **15**, 1(2000).
6. Belle Collaboration, "Measurement of Polarization of  $J/\psi$  in  $B^0 \rightarrow J/\psi + K^{*0}$  and  $B^+ \rightarrow J/\psi + K^{*+}$  Decays," Contributed paper (#285) to the XXXth International Conference on High Energy Physics, July 27 - August 2, 2000, Osaka, Japan. <http://bsunsrv1.kek.jp/conferences/ichep2000.html>